Conference Proceedings

EuroSun 2016

Palma de Mallorca (Spain), 11 – 14 October 2016

Microclimate Mitigation for Reducing Summer Overheating in Historic District

Anna Laura Pisello[1,2], Veronica Lucia Castaldo[1], Cristina Piselli[1], Ilaria Pigliautile[1] and Franco Cotana[1,2]

[1] CIRIAF - Interuniversity Research Center, University of Perugia, Perugia (Italy)

[2] Department of Engineering, University of Perugia, Perugia (Italy)

Abstract

In the context of dense cities, which typically suffer from the Urban Heat Island (UHI) phenomenon, environmental quality is strongly affected by urban design choices and can significantly vary depending on the local boundary conditions and local climate phenomena. In this scenario, the present work analyzes the complex relation between the urban built environment and its local microclimate at neighborhood-urban scale, by means of both experimental field monitoring and numerical analysis. To this aim, an historic urban district in the city center of Perugia (central Italy) was continuously monitored during summer 2015 and the UHI intensity was assessed. Therefore, the validated numerical analysis of the area was carried out through ENVI-met simulation engine in order to quantify the thermal benefits achievable by applying specific tailored mitigations strategies, i.e. green façade, cool roof, and cool pavement, in both summer and winter conditions. The monitoring campaign confirmed that buildings' density and greenery percentage are able to considerably affect outdoor microclimate even in historical districts where the design choices are relatively limited compared to the new urban developments. The numerical analysis highlighted the major role of green façade in generating the most important air temperature drops in a summer day. Moreover, the effectiveness of the proposed mitigation technique is demonstrated also in winter conditions.

Keywords: *Outdoor microclimate, Urban Heat Island, Experimental monitoring, Numerical analysis, Local boundary conditions*

1. Introduction

Nowadays, more than half of the world's population lives in urban districts and it was assessed that in 2050 the 66% of the world's population will be an urban population (United Nations, 2015). This represents a great growth compared to the 30% registered in 1950. For this reason, the necessity to design healthy, efficient, and sustainable built environments is becoming a crucial issue for both designer and urban planners.

As underlined in various studies (Chen and Ng, 2012; Nikolopoulou and Lykoudis, 2006), human outdoor comfort depends on both physiological factors and the thermal conditions of the environment, which have a considerable role in influencing people's usage of urban spaces. Therefore, human thermal comfort has been detected to be one of the most important factors determining the quality of outdoor environments (Lai et al., 2014). One of the main threaten to the quality of urban microclimate is represented by the Urban Heat Island (UHI) phenomenon, which consists in higher air temperatures inside urban areas compared to those of the surrounding rural environment (Mirzaei and Haghighat, 2010). A huge research effort about this local climate phenomenon is carried out with the aim of understating and defining it from both a qualitative and a quantitative point of view. In this view, different approaches have been developed by means of both experimental analyses through in-field measurements and numerical analysis (Mirzaei and Haghighat, 2010). For instance, Papanastasou and Kittas (2012) detected a maximum temperature difference of 3.4 K and 3.1 K

doi:10.18086/eurosun.2016.01.16 Available at http://proceedings.ises.org

in winter and summer, respectively, between the city center and a suburban area of Volos (i.e. a medium-size coastal city in Greece) by comparing data collected from two fixed meteorological stations. Similarly, Mhosin and Gough (2012) assessed the great UHI variability in Toronto, by detecting an increase of about 0.02 K per decade between 1970-2000. On the other hand, mobile surveys were implemented in Padua (Busato et al., 2014) to experimentally characterize the UHI phenomenon. Such approach was able to reveal an UHI up to 6 K inside the city.

UHI is able to influence the weather conditions of a built environment at several scales (Oke, 1976), and the consequences at the urban canopy layer can significantly affect the well-being and health of citizens. Moreover, the global climate change and the increase in frequency and intensity of extreme heat events (Luber and McGeehin, 2008) may contribute in threatening human society even at a local scale, in terms for instance of outdoor visual and thermal comfort for pedestrians (Rosso et al., 2015), human health (McMichael et al., 2006), building energy consumption (Santamouris, 2014b), and also from an economy point of view (Stern and Treasury, 2007). Therefore, the investigation of the complex relationship existing between local variations of urban/suburban microclimate and the built environment could help to (i) reduce the negative effects of the UHI, (ii) find suitable mitigation strategies for each specific urban contest, and (iii) support a sustainable and energy efficient urban planning. In this scenario, Santamouris et al. (2015) showed how a deep knowledge of the microclimate conditions of a city could help to develop specific policy issue and the most appropriate resilience plan to fight the UHI. By using numerical analysis i.e., Teleghani et al. (2014) studied the relationship between the environment configuration and its microclimate by implementing in ENVI-met the model of five simple ideal urban forms. The aim was to provide basic suggestions for urban planners to be easily adapted to realistic situations.

On the contrary, Coronel and Álvarez (2001) found that the ancient neighborhood of Santa Cruz (Seville, Spain) during summer presents better thermal behavior compared to the new areas of the city due to peculiar characteristics of the urban environment, such as diffuse presence of trees and water fountains, high thermal mass of the external walls, mostly white-colored, and aspect ratio and orientation of the narrow streets. In fact, the alteration of local microclimate parameters in built environment is mainly due to a modification of the energy balance inside urban areas which depends on the above mentioned factors, and the presence of anthropogenic heat sources (Giridharan et al., 2007). Over the years different mitigation strategies were demonstrated to be able to improve such energy balance, i.e. the implementation of greenery (Bowler et al., 2010) and high-albedo materials inside built areas (Santamouris, 2014a). Such UHI mitigation techniques have been studied and tested through both experimental and numerical analysis to evaluate their effectiveness (Bruse and Fleer, 1998; Ridder et al., 2004). In the specific context of dense historical cities, Pisello et al. (2015b) tested a combination of these two strategies, since other invasive mitigation techniques cannot be applied due to architectural constraints. Furthermore, in order to overcome such constraints, innovative cool colored coatings were developed to ensure the same esthetic properties of the traditional coatings, but a more selective absorption band in the infrared part of the spectrum. Synnefa et al. (2007) found a maximum temperature difference of 10.2 K between a cool and standard colored coating, and almost the same values were obtained by Pisello et al. (2013) for a clay tile coatings suitable for applications in historic constructions.

2. Motivation

During summer 2015, a monitoring campaign of the outdoor environmental parameters was conducted in four different districts inside the historical city of Perugia, in central Italy. Data collected underlined the presence of higher air temperatures inside the area of the historical city center, which is characterized by dense urban design and lack of green areas. Building upon these finding and previous studies, the purpose of the present work is to investigate the effectiveness of studied suitable strategies to reduce the summer overheating in this context. Therefore, through numerical analysis, green facades, cool roofs, and cool pavements were implemented inside a realistic validated model of the area of interest to assess the benefits achievable in terms of local microclimate parameters and pedestrians' comfort.

Although the main aim is to mitigate summer overheating, microclimate variations were studied also in winter conditions so as to evaluate possible consequences or benefits of the proposed mitigation techniques on outdoor thermal parameters during the cold season.

3. Materials and Methods

In order to pursue the outlined targets, a numerical model of the monitored area within the historical center of Perugia during summer 2015 (Fig. 1a) was developed. To ensure the reliability of simulation results, a (i) preliminary phase of validation was conducted. Once reached an acceptable correspondence between measured and simulated data, (ii) alternative scenarios to the real one (with well-acknowledged mitigation strategies), were simulated during a summer and a winter day. More in detail, the daily weather profiles were selected from the typical July (July, 15^{th}) and typical January (January, 15^{th}) provided by IGDG TMY (Typical Meteorological Year) for the city of Perugia, built on 1951-1970 period of record (U.S. Department of Energy, 2014). Therefore, (iii) the microclimate output obtained from the simulation were analyzed in terms of the outdoor thermal comfort index PET (Physiological Equivalent Temperature) (Chirag and Ramachandraiah, 2010) to assess how these mitigation strategies could affect pedestrian perception of the surrounding environment (Fig. 1).

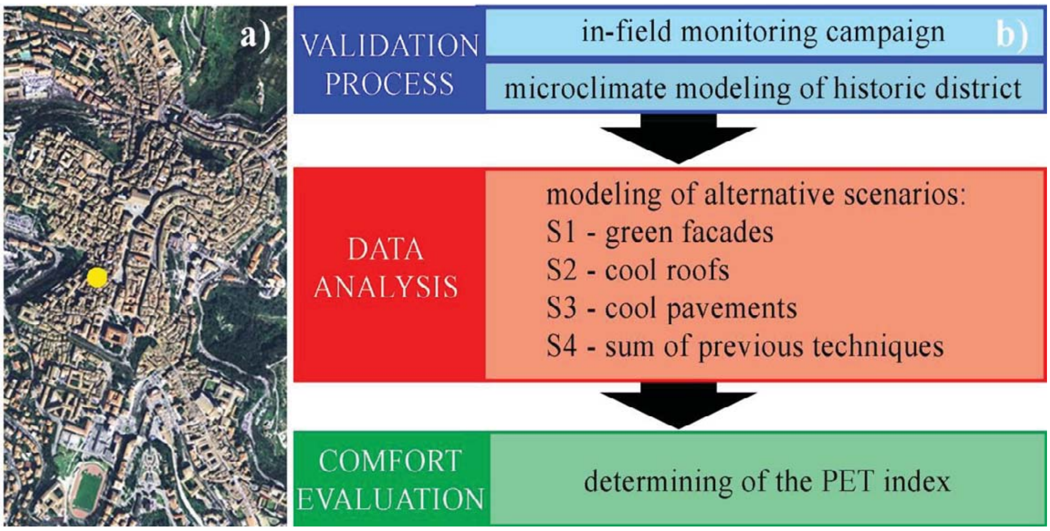

Fig. 1: (a) Position of the modeled area within the historic center of Perugia and (b) scheme of the adopted methodology

3.1. Modeling and validation process

The studied area is an East-West oriented street, 40 m long with a width varying from 3 to 12 m along its length (Fig. 2). Moreover, between the eastern and western side there is a height difference of 5 m. As the area is located in the historical center of the city, buildings surrounding the street are characterized by thick stone walls and the outdoor pavements are covered by bricks and plates made of *pietra serena* (except for the final western side which was recently asphalted) (Fig. 2c).

A three-dimensional microclimate modeling system, i.e. within ENVI-met V4 environment, designed to simulate the surface-plant-air interactions with a resolution from 0.5 to 10 m in space and from 1 to 5 sec in time, was used for the numerical analysis (Huttner and Bruse, 2009). The choice of the software was related to the high accuracy in space provided, which is optimal to study urban microclimate at a low scale, i.e. within the Urban Canopy Layer, where this work is focused. A realistic model of the area was developed and calibrated by using experimental data collected during the summer 2015 monitoring campaign. The calibration was performed following the suggestions of the ASHRAE GUIDELINE 14-2002 (ASHRAE, 2005), through both a statistical and graphical approach. The geometrical base of the model is a 3D grid of dimensions 30x60x35 having 1m side cube as unit. The materials used to characterize walls, roofs, and pavements were selected from the software database and their thermo-physical properties are summarized in Tables 1 and 2.

In order to have the necessary data for the calibration, during the monitoring campaign a portable weather station placed at 15 m height (Pisello et al., 2014) and two Tinytag temperature and relative humidity probes and data-loggers (Pisello et al., 2015a) located at 2 m above the ground (Fig. 2d) were installed. As weather input the following data were used:

- Initial wind speed: value collected from the weather station at 6 a.m., start time of the simulation;
- Wind direction: value prevailing during the three days of the monitoring campaign;
- 24h air temperature and relative humidity forcing: data collected by the probe located on the South-oriented side (Fig. 2d, point B).

The simulation has been running for 24h and the data comparison for the calibration corresponded to those collected from the North-oriented probe (Fig. 2d, point A) and those extracted from its representative point within the model.

Fig. 2: View of the street from the (a) western and (b) eastern sides, (c) view of the street crossing the studied one on the East, and (d) localization in the plant of the monitoring probes

Tab. 1: Characteristics of the walls and roofs composing the reference scenario

Element	Albedo [-]	Emittance [-]	Specific heat [J/kg·K]	Thermal conductivity [W/m·K]	Density [kg/m^3]
Walls	0.30	0.90	840	0.86	930
Roofs	0.50	0.90	800	0.84	1900

Tab. 2: Characteristics of the different pavement profiles composing the reference scenario

Pavement profile	Albedo [-]	Emittance [-]	Volumetric Heat Capacity (upper layer) [J/m^3·K]	Heat Conductivity (upper layer) [W/m·K]
Brick Road	0.30	0.90	$2.00 \cdot 10^6$	1.00
Basalt Brick Road	0.80	0.90	$2.39 \cdot 10^6$	1.73
Asphalt Road	0.20	0.90	$2.25 \cdot 10^6$	0.90

3.2. Modeling of alternative scenarios

Alternative scenarios to the reference one, named S0, were developed by modeling the application at urban level of the following strategies for Urban Heat Island mitigation:

- Increase of urban greenery: introduction of vertical green systems on the buildings' facades, i.e. scenario S1;

- Replacement of traditional materials with high-reflectance ones: highly reflective roofs, i.e. scenario S2, and pavements, i.e. scenario S3, developed by using cool solutions for the coating material;
- Combination of the three mitigation strategies, i.e. scenario S4.

All the strategies, as summarized in Table 3, were selected to be realistically implemented in the case study area, which presents architectural constrains since it is located inside the historical center of the city. In particular, cool materials characterized by the same spectral response of traditional ones in the only visible region were considered in order to preserve buildings' heritage value, while providing higher reflectance values in the other ranges of the solar spectrum (Pisello et al., 2013). Moreover, pavement's thermal properties were optimized based on the real necessity to substitute the current asphalt area. The last technique, i.e. green façade, can be well integrated with the existing context as it is already installed in a building facing the crossing street (Figure 2c).

Tab. 3: Characteristics of the components modified in each mitigation scenario

Scenario	Element	Mitigation technique	Properties
S1	Walls' Façade	Greenery	Leaf Area Density: 2 m^2/m^3 Foliage albedo: 0.60
S2	Roofs	Cool material	Albedo: 0.75
S3	Pavement	Cool material	Albedo: 0.85
S4	Combination of all the above mentioned techniques		

The five scenarios were simulated during a representative summer and winter day in the climate context of Perugia, Italy, by using as weather input the TMY weather files for the months of July and January, respectively.

3.3. Outdoor thermal comfort analysis of mitigation scenarios

In order to evaluate the benefits achieved through the implementation of the mitigation strategies, the weather data obtained as output in the numerical simulation were analyzed in terms of thermal comfort improvements inducted in the surrounding outdoor area. A comparison between data obtained in the reference and alternative scenarios was performed by analyzing (i) the spatial distribution of the environmental parameters through describing maps and (ii) their variation in time during the day. Maps were generated when air temperature reaches its maximum value (i.e. 3:00 p.m.) and just after the sunset (i.e. 9:00 p.m.). Time series were extracted at 1.5 m, i.e. pedestrian level, from the ground in two different points selected because of their different characteristics (Fig. 3).

Furthermore, the Physiological Equivalent Temperature (PET) was chosen as the parameter representative of the outdoor comfort of pedestrians. The index was evaluated through RayMan data post-process software (Matzarakis et al., 2007).

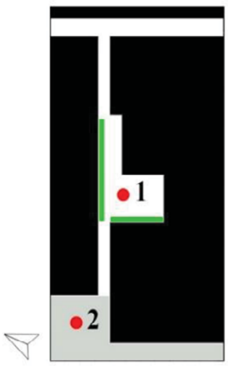

	Location	SVF	Time range when reached by direct solar radiation
Point 1 [x=12, y=28, z=5]	3 and 4 m distant from the east-west and the north-south oriented green walls, respectively	0.15	12:00-2:00 p.m.
Point 2 [x=5, y=8, z=1]	above the area originally presenting pavement made by asphalt	0.51	3:00-8:00 p.m.

location of green facades
asphalted area

Fig. 3: Location in the model of the two points selected to extract simulation data (at 1.5 m height)

4. Results and Discussion

4.1. Model calibration

The graphical and statistical approach followed for the model calibration was carried out as suggested by the ASHRAE GUIDELINE 14 (ASHRAE, 2005). The results depicted in Fig.4 show that the difference in terms of air temperature, between the measured and simulated values, is always lower than 3 K and mostly lower than 1 K. The maximum gap is reached during the hottest hours of the day, when the software tends to overestimate this parameter. Moreover, the difference in terms of air relative humidity is always lower than 10 %.

In addition to the graphical analysis presented in Fig. 4, two statistical indexes, i.e. *Mean Bias Error* (MBE) and *Root Mean Square Error* (RMSE) (ASHRAE, 2005), were evaluated, as reported in Table 4. According to the obtained results, the model can be considered representative of the real area with good approximation. Therefore, it can be used to simulate which could be the improvements in the outdoor microclimate of the zone due to the application of the selected mitigation strategies.

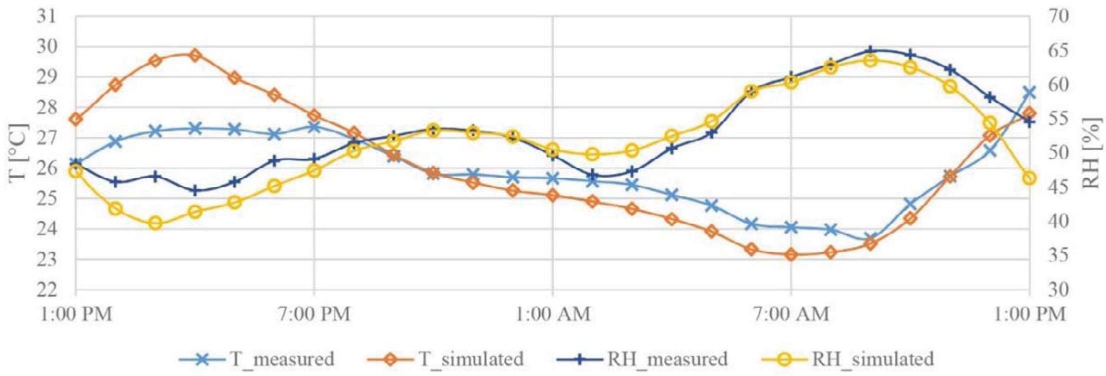

Fig. 4: Comparison of measured and simulated air temperature and relative humidity values trend for model validation

Tab. 4: Calibration parameters results

Parameter	MBE	RMSE
Air Temperature	0.82 K	1.05 K
Relative Humidity	2.21 %	2.96 %

4.2. Summer analysis

The analysis of the alternative simulated scenarios shows that, as expected, scenario S4, combining all the mitigation solutions, is the most advantageous one in summer (July, 15th) in terms of air temperature reduction, especially at pedestrian level (Fig. 5). In fact, by examining the air temperature values in the two analyzed positions, a decreasing trend is detected in the daytime. The best improvement is achieved at point 2, the one located in the previously asphalted area, where an air temperature decrease is registered during all the daytime, varying from -0.5 K (at 8:00 a.m.) to -0.85 K (at 3:00 p.m.).

By analyzing each strategy contribution, the implementation of greenery (S1) seems to be the most effective solution. Moreover, this strategy is the only one leading to benefits in both the points selected. However, in the point closest to the green façade (point 1) the maximum cooling, equal to -0.36 K, is obtained at around 3:00 p.m., i.e. in the peak temperature hours. Whereas, in point 2 the cooling benefit is not perceived during the daytime and the maximum cooling (about 0.4 K) is reached during the coolest hours, i.e. at around midnight, given the different exposition to direct solar radiation of the two points and the reduced heat emission from the walls due to the presence of greenery.

Opposite results, but similar behavior, are detected in S2, where high reflectance tiles are applied on the building roof. In both the points the air temperature increases during the daytime if compared to the reference scenario, especially in point 2. However, these worst values registered in presence of solar radiation (the maximum increment of air temperature, equal to +0.21 K, is found at 7:00 p.m.) are balanced by improvements obtained during the night, leading to a difference up to -0.26 K at 6:00 a.m. This effect is due to the lower surface temperatures of the built surfaces and, therefore, to their lower contribution in the thermal balance during the nighttime.

Unlike previous results, a different behavior can be noticed in scenario S3, where the pavement reflectance is increased. In particular, in point 2 a drop in temperature is registered during the whole day leading to a mean daily reduction equal to -0.29 K, compared to the reference scenario, i.e. S0. On the other hand, at point 1 the temperature values are slightly increased from 12:00 to 7:00 p.m., with negligible differences up to +0.04 K (at 2:00 p.m.). In fact, point 2 is located above the ground surface covered by asphalt in the reference configuration and, therefore, the thermal properties improvement of the proposed materials are mostly perceived. On the contrary, point 1 seems to suffer from the presence of solar radiation, both direct and diffuse, since it is reached by higher mutual reflections of short wave radiation from the surrounding structures.

The relative humidity trend is strictly connected to the air temperature. However, relevant differences can be noticed just in scenarios S1 and S4 where greenery acts like a vapor source due to plants transpiration. The ratio between the ΔT and ΔRH is detected to be around -0.32 in the scenarios without greenery, but gets lower (-0.19 at point 1, the closer to the green facades, and -0.25 at point 2) after the introduction of vegetation.

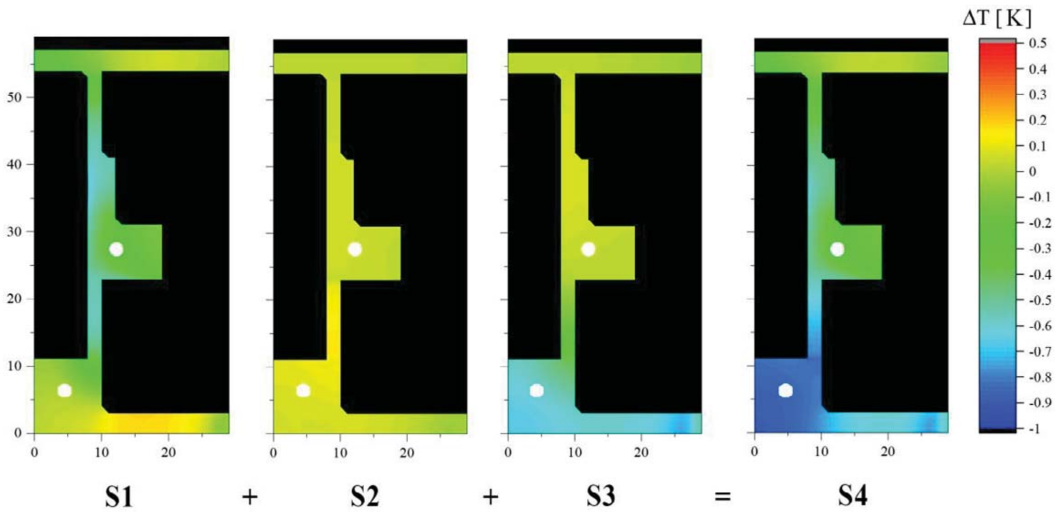

Fig. 5: Air temperature difference between reference (S0) and different mitigation scenarios in the summer day at 3:00 p.m.

Furthermore, the mean radiant temperature (MRT) values were analyzed (Fig. 6). The trend of the MRT shows one peak at point 1, while two peaks at point 2, since direct solar radiation occurs at different times in the two selected locations. At point 1, the peak coincides with the maximum values of reflected solar radiation (at around 1:00 p.m.). At point 2, a first relative peak is detected due to the maximum value of reflected radiation and an additional one is achieved at 3:00 p.m., when the point is reached for the first time by direct solar radiation. Additionally, unlike the previous results in terms of air temperature, the scenario S4 shows worst MRT values with respect to S0, and the solution which mostly influences this effect is the cool paving, i.e. scenario S3. In fact, the pavement reflectance, where high-albedo materials are applied, is able to significantly affect this parameter. Therefore, in the new comprehensive solution S4, a higher mean radiant temperature is observed during the daytime with respect to S0. Although this behavior is registered in both points, a wider range of values is detected in point 2, where MRT achieves its worst value (i.e. +7.62 K at 1:00 p.m.). However, it maintains lower values during the night (mean nighttime increase of +0.1 K) if compared to point 1 (mean nighttime increase of +1.5 K), where the SVF is lower. This is also the reason why in S4 an enhancement of the MRT, i.e. up to -0.11 K, is registered after sunset only in point 2.

An opposite behavior, but with relatively minor impact on the final results, is detected for S2, where modification of buildings' roof reflectance properties are implemented by increasing the albedo of a 50% (i.e. from 0.5 to 0.75). In this scenario, the wider temperature variation is registered in point 1, from a minimum of -0.9 K at 8:00 a.m. up to a maximum of +0.8 K at 8:00 p.m., while in point 2 the range is between -0.55 K and +0.42 K.

Finally, benefits are registered also in terms of MRT by comparing the scenario characterized by the presence of greenery, i.e. S1, and S0. In detail, at point 1, which is closer to the green façade, lower values of MRT are detected, compared to S0, for almost all the daytime reaching a maximum of -2.84 K at 2:00 p.m. Therefore, an average daily reduction of MRT equal to -0.28 K is detected. Similar but lower effect is registered at point 2, where the achieved mean daily drop of MRT is equal to -0.21 K.

In order to assess the effect of the proposed strategies on the outdoor thermal comfort conditions, the PET index was calculated for the different scenarios (Fig. 7). The PET is strictly related to the trend of the mean radiant temperature, and it was obtained by imposing a clo (static clothing insulation) equal to 0.5. Results show how the midday MRT increase due to the implementation of the high reflective paving causes the increase of the PET in scenario S3 and S4 when the two points are reached by the direct solar radiation and when the peak of reflected solar radiation occurs. Whereas, the pedestrian comfort is improved in particular in point 1 due to the positive effect of the green facades.

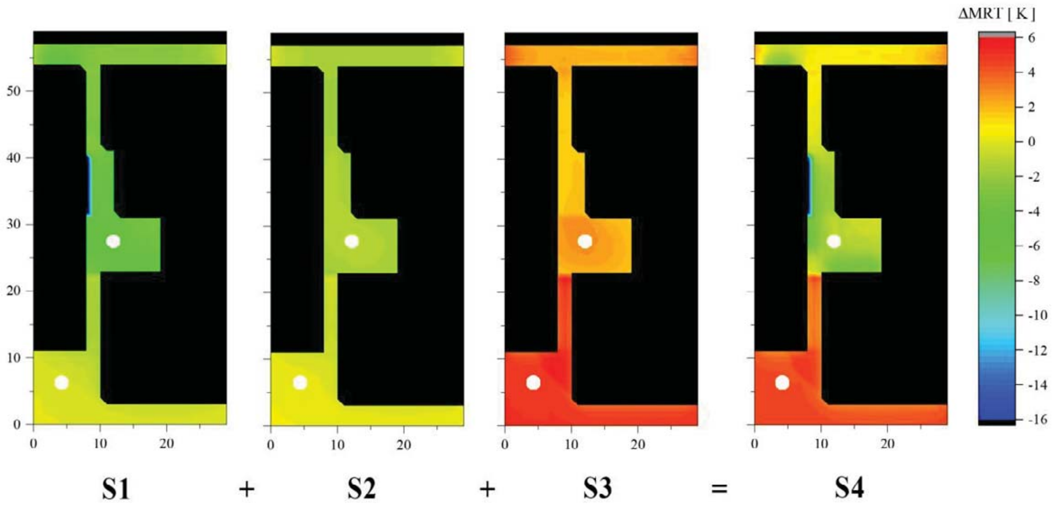

Fig. 6: Mean radiant temperature difference between reference (S0) and different mitigation scenarios in the summer day at 3:00 p.m.

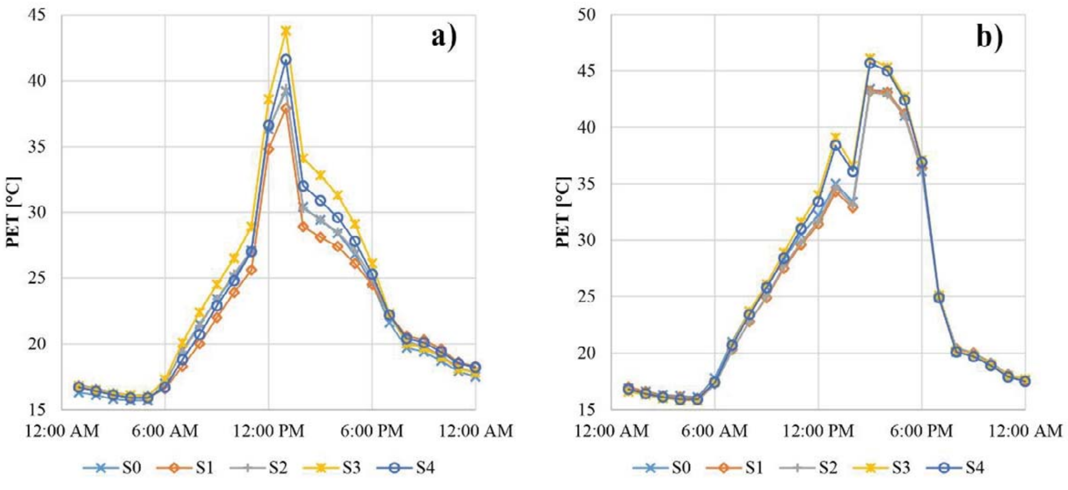

Fig. 7: PET daily trend in all simulated scenarios at (a) point 1 and (b) point 2 in the summer day

4.3. Winter analysis

Even if the proposed mitigation techniques are specifically designed to improve the outdoor thermal comfort conditions of the case study area during the hottest season (when the worst conditions in terms of outdoor thermal comfort are experienced at these latitudes), this section describes the results of the analysis of their effects during winter (January, 15th). The aim is to evaluate if the thermal comfort could be enhanced also in the cold season, or at least not reduced, and to quantify the potential benefits of the applied strategies, which are expected to be lower, compared to the summer ones.

In terms of air temperature, low improvements were detected in almost all the scenarios (Fig. 8). The only exception is registered in S3, i.e. in presence of high reflectance pavements, at point 2 from 12:00 to 4:00 p.m. However, a maximum decreasing of air temperature of only -0.06 K is detected at 2:00 p.m., meaning that paving surfaces are reaching lower surface temperatures even if subjected to the same direct radiation (as expected for cool materials). Nevertheless, S3 is globally the scenario where the higher air temperature increase is detected, with a mean daily variation, of +0.10 K at point 2 with respect to the reference scenario (S0). Instead, at point 1 the maximum mean daily variation, equal to +0.08 K, is registered in S1, i.e. where green facades are implemented. Moreover, higher air temperature improvements occur during the nighttime, when the lowest values of the parameter are reached.

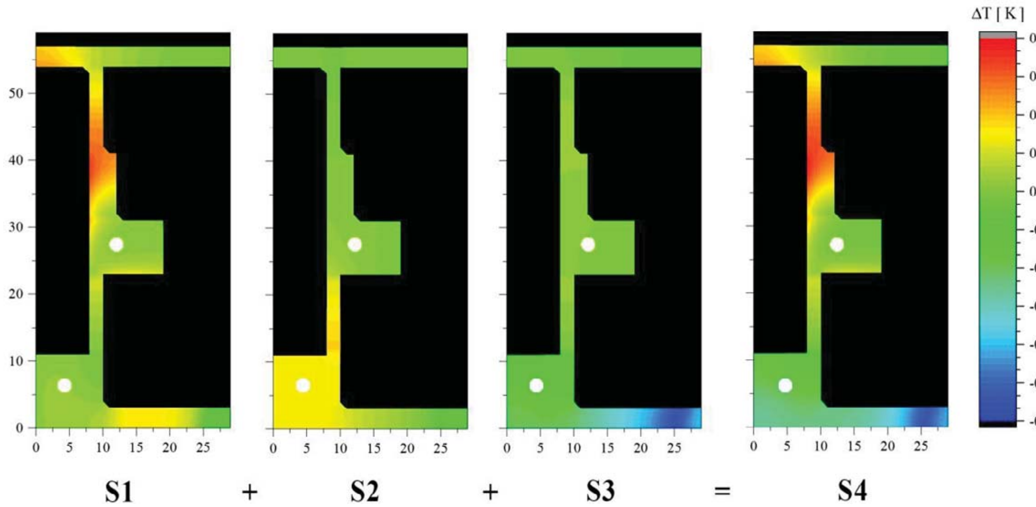

Fig. 8: Air temperature difference between reference (S0) and different mitigation scenarios in the winter day at 3:00 p.m.

Greater variations were found in terms of mean radiant temperature (Fig. 9), in particular at point 1, the one presenting the lower value of SVF (i.e 0.15). In fact, during winter both the selected points are never reached by direct solar radiation, due to the lower height of sun in this season. Therefore, in the absence of direct solar radiation, the effect of mutual reflectance between built surfaces has a stronger impact on the MRT. The highest values of the MRT occur in S3 (characterized by cool pavements) where a maximum difference of +3.41 K, compared to the reference scenario, is detected at 2:00 p.m., i.e. when the reflected radiation reaches its maximum. On the other hand, the introduction of greenery, i.e. S1, causes a drop in the MRT equal to -2.12 K in point 1, where the presence of the green vertical system is more perceived. After the sunset (i.e. at 5:00 p.m.) the effect of all mitigation strategies is almost the same and vary from +2.93 K (i.e. in S1) to +4.00 K (i.e. in S3) at point 1, and from +1.54 K (i.e. S1) to +2.32 K (i.e. S3) at point 2.

As regards the outdoor comfort assessment, the PET (Fig.10) was evaluated also in winter conditions by imposing a cloth resistance of 1.2 clo. In general, although the improvements are detected to be low, apart for S3, it is interesting to notice that the PET gap between the improved scenarios and the reference one is more significant in the nighttime rather than during the day. It means that the applied strategies induce an increment in terms of PET especially in the coldest hours. Therefore, even if the proposed solutions were specifically designed to fight discomfort conditions during the hot season, their effect is non-negligible also during winter, even if less significant.

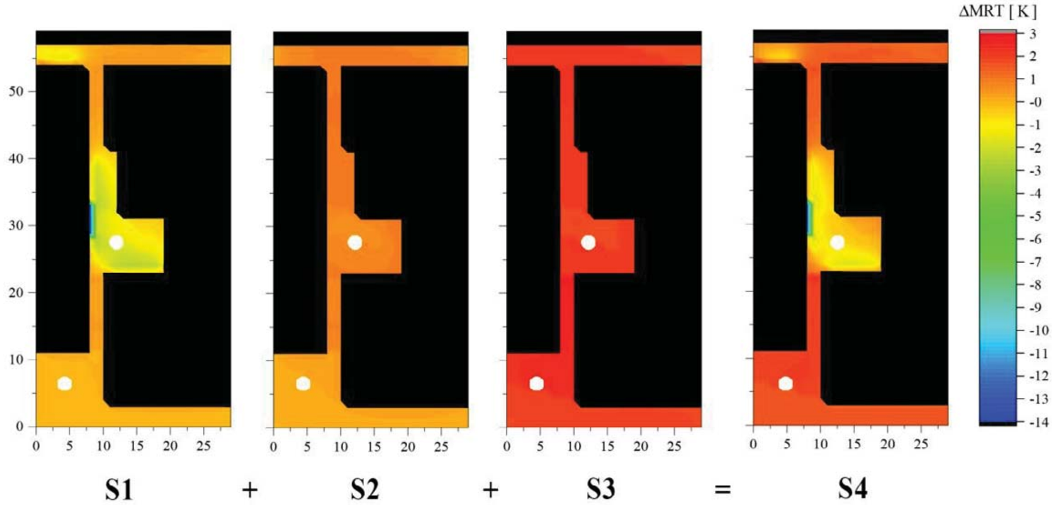

Fig. 9: Mean radiant temperature difference between reference (S0) and different mitigation scenarios in the winter day at 3:00 p.m.

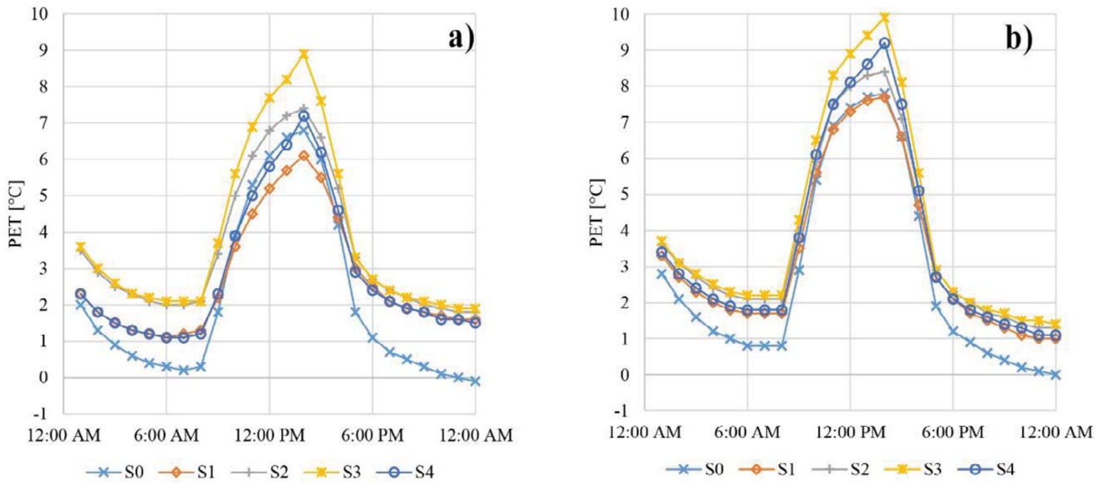

Fig. 10: PET daily trend in all simulated scenarios at (a) point 1 and (b) point 2 in the winter day

5. Conclusions

Urban microclimate has a strong influence on many aspects of human life in the cities. In dense urban environments, the Urban Heat Island phenomenon is a threat to the quality and the livability of the outdoor built environment. In this work, the impact of different UHI mitigation strategies implemented within a real historical precinct was assessed through calibrated numerical analysis, i.e. by using ENVI-met V4. Four possible mitigation scenarios were evaluated under both summer and winter conditions, i.e. the implementation of (i) greenery on building facades, (ii) cool roofs, (iii) cool pavements, and (iv) the combination of these three strategies. The possible thermal benefits deriving from their application were quantified in terms of microclimate parameters and outdoor comfort index, i.e. PET.

Generally, results showed improvements in terms of air temperature for all the solutions both during a summer and a winter day. The implementation of greenery led to the greater temperature gaps in summer, with respect to the reference scenario, i.e. an average daily difference (calculated for the whole analyzed area) of -0.25 K (at 1 m height) compared to the -0.05 K and -0.18 K obtained by implementing cool roofs and cool pavements, respectively. Whereas in winter, when lower effects were registered, no strong differences were noticed among the different scenarios. Furthermore, greenery was the only solution that improved the radiative balance of the outdoor environment in summer. On the contrary, the implementation of cool materials, and in particular of cool pavements, caused a huge increase of the mean radiant temperature, which negatively affected the human thermal perception of the outdoor space in summer.

Future developments of this work will analyze the effects of such mitigation strategies applied diffusely within the city, enlarging the area of study. The final aim will be to provide reliable information to support both designers and urban planners in the design and development of policies to improve dwellers and pedestrians' quality of life.

References

ASHRAE, 2005. ASHRAE's Guideline 14-2002 for Measurement of Energy and Demand Savings: How to Determine What was Really Saved by the Retrofit. American Society of Heating, Refrigerating and Air-Conditioning Engineers, Atlanta, GA.

Bowler, D.E., Buyung-Ali, L., Knight, T.M., Pullin, A.S., 2010. Urban greening to cool towns and cities: A systematic review of the empirical evidence. Landsc. Urban Plan. 97, 147-155.

Bruse, M., Fleer, H., 1998. Simulating surface–plant–air interactions inside urban environments with a three dimensional numerical model. Environ. Model. Softw. 13, 373-384.

Busato, F., Lazzarin, R.M., Noro, M., 2014. Three years of study of the Urban Heat Island in Padua: Experimental results. Sustain. Cities Soc. 10, 251-258.

Chen, L., Ng, E., 2012. Outdoor thermal comfort and outdoor activities: A review of research in the past decade. Cities 29, 118-125.

Chirag, D., Ramachandraiah, A., 2010. The significance of Physiological Equivalent Temperature (PET) in outdoor thermal comfort studies. Int. J. of Eng. Sci. Te. 2 (7), 2825-2828.

Coronel, J.F., Álvarez, S., 2001. Experimental work and analysis of confined urban spaces. Sol. Energy 70 (3), 263-273.

De Ridder, K., Adamec, V., Bañuelos, A., Bruse, M., Bürger, M., Damsgaard, O., Dufekb, J., Hirschf, J., Lefebrea, F., Pérez-Lacorzanac, J.M., Thierrye, A., Weberf, C., 2004. An integrated methodology to assess the benefits of urban green space. Sci. Total Environ. 334-335, 489-497.

Giridharan, R., Lau, S.S.Y., Ganesan, S., Givoni, B., 2007. Urban design factors influencing heat island intensity in high-rise high-density environments of Hong Kong. Build. Environ. 42 (10), 3669-3684.

Huttner, S., Bruse, M., 2009. Numerical modeling of the urban climate – A preview on ENVI-MET 4.0. The seventh International Conference on Urban Climate, 29 June-3 July 2009, Yokohama, Japan. <http://www.envi-met.com/documents/papers/ICUC7_ModellingV4.pdf>.

Lai, D., Zhou, C., Huang, J., Jiang, Y., Long, Z., Chen, Q., 2014. Outdoor space quality: A field study in an urban residential community in central China. Energ. Buildings 68, 713-720.

Luber, G. McGeehin, M., 2008. Climate Change and Extreme Heat Events. Am. J. Prev. Med. 35, 429-435.

Matzarakis, A., Rutz, F., Mayer, H., 2007. Modelling radiation fluxes in simple and complex environments-application of the RayMan model. Int. J. Biometeorol. 51, 323-334.

McMichael, A.J., Woodruff, R.E., Hales, S., 2006. Climate change and human health: present and future risks. Lancet. 367, 859-869.

Mirzaei, P.A., Haghighat, F., 2010. Approaches to study Urban Heat Island – Abilities and limitations, Build. Environ. 45, 2192-2201.

Mohsin, T., Gough, W.A., 2012. Characterization and estimation of urban heat island at Toronto: Impact of the choice of rural sites. Theor. Appl. Climatol. 108, 105-117.

Nikolopoulou, M., Lykoudis, S., 2006. Thermal comfort in outdoor urban spaces: Analysis across different European countries. Build. Environ. 41, 1455-1470.

Oke, T.R., 1976. The distinction between canopy and boundary layer urban heat islands. Atmosphere 14, 268-277.

Papanastasiou, D.K., Kittas, C., 2012. Maximum urban heat island intensity in a medium/sized coastal Mediterranean city. Theor. Appl. Climatol. 107, 407-416.

Pisello, A.L., Cotana, F., Nicolini, A., Brinchi, L., 2013. Development of clay tile coatings for steep-sloped cool roofs. Energies 6, 3637-3653.

Pisello, A.L., Cotana, F., Nicolini, A., Buratti, C., 2014. Effect of dynamic characteristics of building envelope on thermal-energy performance in winter conditions: In field experiment. Energ. Buildings 80, 218-230.

Pisello, A.L., Pignatta, G., Castaldo, V.L., Cotana, F., 2015a. The impact of local microclimate boundary conditions on building energy performance. Sustainability 7 (7), 9207-9230.

Pisello, A.L., Piselli, C., Cotana, F., 2015b. Thermal-physics and energy performance of an innovative green roof system: The Cool-Green Roof. Sol. Energy 116, 337-356.

Rosso, F., Pisello, A.L., Pignatta, G., Castaldo, V.L., Piselli, C., Cotana, F., Ferrero, M., 2015. Outdoor Thermal and Visual Perception of Natural Cool Materials for Roof and Urban Paving. Procedia Eng. 118, 1325-1332.

Santamouris, M., 2014a. Cooling the cities – A review of reflective and green roof mitigation technologies to fight heat island and improve comfort in urban environments. Sol. Energy 103, 682-703.

Santamouris, M., 2014b. On the energy impact of urban heat island and global warming on buildings. Energ. Buildings 82, 100-113.

Santamouris, M., Cartalis, C., Synnefa, A., 2015. Local urban warming, possible impacts and a resilience plan to climate change for the historical center of Athens, Greece. Sustain. Cities Soc. 19, 281-291.

Synnefa, A., Santamouris, M., Apostolakis, K., 2007. On the development, optical properties and thermal performance of cool colored coatings for the urban environment. Sol. Energy 81, 488-497.

Stern, N.H., Treasury, G.B., 2007. The economics of climate change: the Stern review, Cambridge University Press.

Taleghani, M., Kleerekoper, L., Tenpierik, M., van den Dobbelsteen, A., 2014. Outdoor thermal comfort within five different urban forms in the Netherlands. Build. Environ. 83, 65-78.

United Nations, Department of Economic and Social Affairs, Population Division, 2015. World Urbanization Prospects: The 2014 Revision. <https://esa.un.org/unpd/wup/Publications/Files/WUP2014-Report.pdf>.

U.S. Department of Energy, Energy Efficiency and Renewable Energy, 2014. <http://apps1.eere.energy.gov/buildings/energyplus/cfm/weather_data3.cfm/region=6_europe_wmo_region_6/country=ITA/cname=Italy>, WMO Station Region 6: Italy, Perugia 161810 (IGDG).